Article

Cell

Sugar Synthesis from CO_2 in *Escherichia coli*

Graphical Abstract

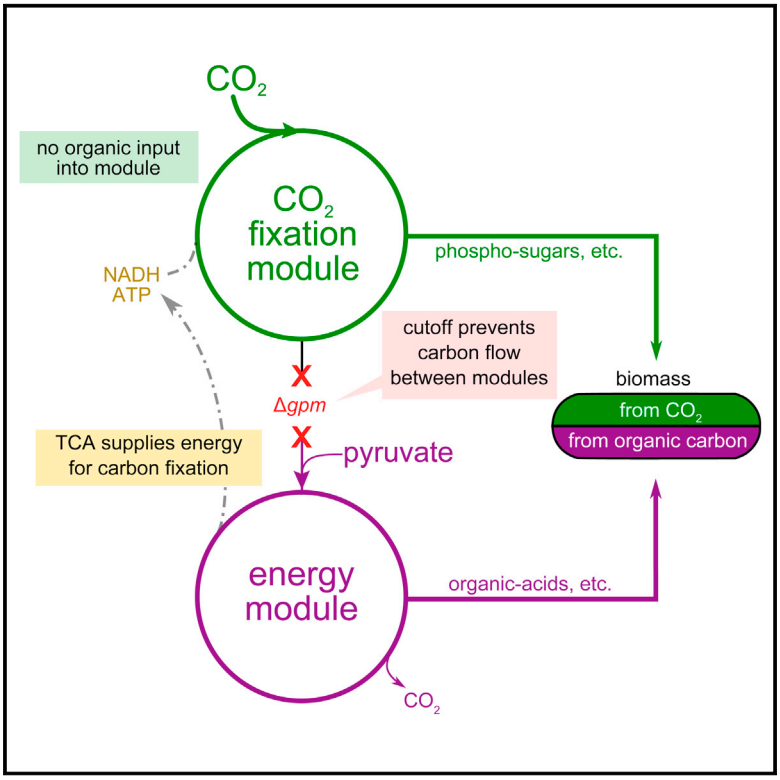

Authors

Niv Antonovsky, Shmuel Gleizer, Elad Noor, ..., Ghil Jona, Arren Bar-Even, Ron Milo

Correspondence

ron.milo@weizmann.ac.il

In Brief

Metabolic rewiring and directed evolution lead to a fully functional, non-native carbon fixation cycle, which synthesizes sugars and other major biomass components in *E. coli.*

Highlights

- Non-native Calvin-Benson cycle allows for sugar synthesis from CO_2 in *E. coli*
- Metabolic cutoff allows for the decoupling of energy harvesting from biomass synthesis
- Chemostat-based directed evolution led to the emergence of sugar synthesis from CO_2
- Mutations in flux branchpoints are essential for the CBB cycle stable operation

Antonovsky et al., 2016, Cell *166*, 1–11
June 30, 2016
http://dx.doi.org/10.1016/j.cell.2016.05.064

CellPress

Please cite this article in press as: Antonovsky et al., Sugar Synthesis from CO_2 in *Escherichia coli*, Cell (2016), http://dx.doi.org/10.1016/j.cell.2016.05.064

Article

Cell

Sugar Synthesis from CO_2 in *Escherichia coli*

Niv Antonovsky,[1] Shmuel Gleizer,[1] Elad Noor,[1] Yehudit Zohar,[1] Elad Herz,[1] Uri Barenholz,[1] Lior Zelcbuch,[1] Shira Amram,[1] Aryeh Wides,[1] Naama Tepper,[2] Dan Davidi,[1] Yinon Bar-On,[1] Tasneem Bareia,[1] David G. Wernick,[1] Ido Shani,[1] Sergey Malitsky,[1] Ghil Jona,[3] Arren Bar-Even,[1] and Ron Milo[1,*]

[1]Department of Plant and Environmental Sciences, Weizmann Institute of Science, Rehovot 7610001, Israel

[2]Department of Computer Science, Technion, Israel Institute of Technology, Haifa 3200003, Israel

[3]Department of Biological Services, Weizmann Institute of Science, Rehovot 7610001, Israel

*Correspondence: ron.milo@weizmann.ac.il

http://dx.doi.org/10.1016/j.cell.2016.05.064

SUMMARY

Can a heterotrophic organism be evolved to synthesize biomass from CO_2 directly? So far, non-native carbon fixation in which biomass precursors are synthesized solely from CO_2 has remained an elusive grand challenge. Here, we demonstrate how a combination of rational metabolic rewiring, recombinant expression, and laboratory evolution has led to the biosynthesis of sugars and other major biomass constituents by a fully functional Calvin-Benson-Bassham (CBB) cycle in *E. coli*. In the evolved bacteria, carbon fixation is performed via a non-native CBB cycle, while reducing power and energy are obtained by oxidizing a supplied organic compound (e.g., pyruvate). Genome sequencing reveals that mutations in flux branchpoints, connecting the non-native CBB cycle to biosynthetic pathways, are essential for this phenotype. The successful evolution of a non-native carbon fixation pathway, though not yet resulting in net carbon gain, strikingly demonstrates the capacity for rapid trophic-mode evolution of metabolism applicable to biotechnology.

INTRODUCTION

Whether CO_2 can or cannot be transformed into sugar and biomass by carbon fixation is arguably the most basic distinction we make in defining the metabolism of an organism. Carbon fixation by autotrophs is the biochemical gateway to the organic world, as obligate heterotrophs are dependent on this supply of organic carbon. How difficult is it to evolve from one trophic mode of growth to another? Specifically, can the ability to synthesize biomass from CO_2 be introduced into a heterotrophic organism? Exploring the process in which a heterotrophic bacterium, such as *Escherichia coli*, is evolved to synthesize sugars from CO_2 can serve as a model system to tackle these questions.

The utilization of one-carbon compounds, such as CO_2, methanol, and methane, has been recently drawing attention as a low-cost, abundant feedstock option for biochemical production (Li et al., 2012; Müller et al., 2015; Siegel et al., 2015). Recent studies have demonstrated that a wide variety of non-native metabolic pathways can be integrated into model microorganisms, allowing the synthesis of value-added chemicals using sugar as a feedstock (Galanie et al., 2015; Yim et al., 2011). However, efforts to synthesize sugar from inorganic CO_2 by introducing a non-native carbon fixation cycle have never been successful. Carbohydrate biosynthesis through carbon fixation in *E. coli* would not only open exciting avenues to directly utilize CO_2 for chemical production, but could also serve as a platform to rapidly optimize carbon fixation enzymes and pathways for subsequent implementation in agricultural crops (Lin et al., 2014; Mueller-Cajar and Whitney, 2008; Parikh et al., 2006; Shih et al., 2014). Furthermore, this experimental approach could shed light on cellular adaptations associated with horizontal-gene-transfer events, on the plasticity of metabolic networks, and on the evolutionary emergence of a biological novelty.

The achievement of novel biological phenotypes on laboratory timescales is at the heart of efforts such as the long-term evolutionary experiment, which studied how *E. coli* developed the ability to utilize citrate throughout several tens of thousands of generations (Blount et al., 2008; Maddamsetti et al., 2015; Wiser et al., 2013). These studies show the intricate dynamics of potentiating, actualizing, and refining steps during the evolutionary process (Quandt et al., 2015) and shed light on the interplay between selection, historical contingency, and epistatic effects. In parallel to lab evolution, which forces the selective conditions, synthetic biology efforts manipulate the genetic makeup with the aim of rationally designing desired phenotypes (Church et al., 2014; Galanie et al., 2015). In spite of significant progress, nothing as extreme as expressing a fully functional pathway that changes the trophic mode of an organism has been ever shown to be achievable.

The Calvin-Benson-Bassham cycle (Bassham et al., 1954) is, by far, the most dominant carbon fixation pathway in the biosphere out of all six known natural alternatives (Fuchs, 2011; Bar-Even et al., 2012). Previous efforts to show functional expression of the CBB cycle carboxylating enzyme, ribulose-1,5-bisphosphate carboxylase/oxygenase (RuBisCO), in *E. coli* have relied on the supply of a glycolytic carbon source (e.g., glucose) to replenish RuBisCO's substrate, ribulose-bisphosphate (RuBP) (Durão et al., 2015; Gong et al., 2015; Mueller-Cajar and Whitney, 2008; Parikh et al., 2006; Zhuang and Li, 2013). These important studies therefore did not achieve the defining function of the CBB cycle of autocatalytic sugar synthesis from inorganic carbon. While this approach led to the elegant construction of a RuBisCO-dependent *E. coli* as a platform for directed evolution of RuBisCO activity (Durão et al., 2015; Mueller-Cajar and Whitney, 2008; Parikh et al., 2006), evolving a

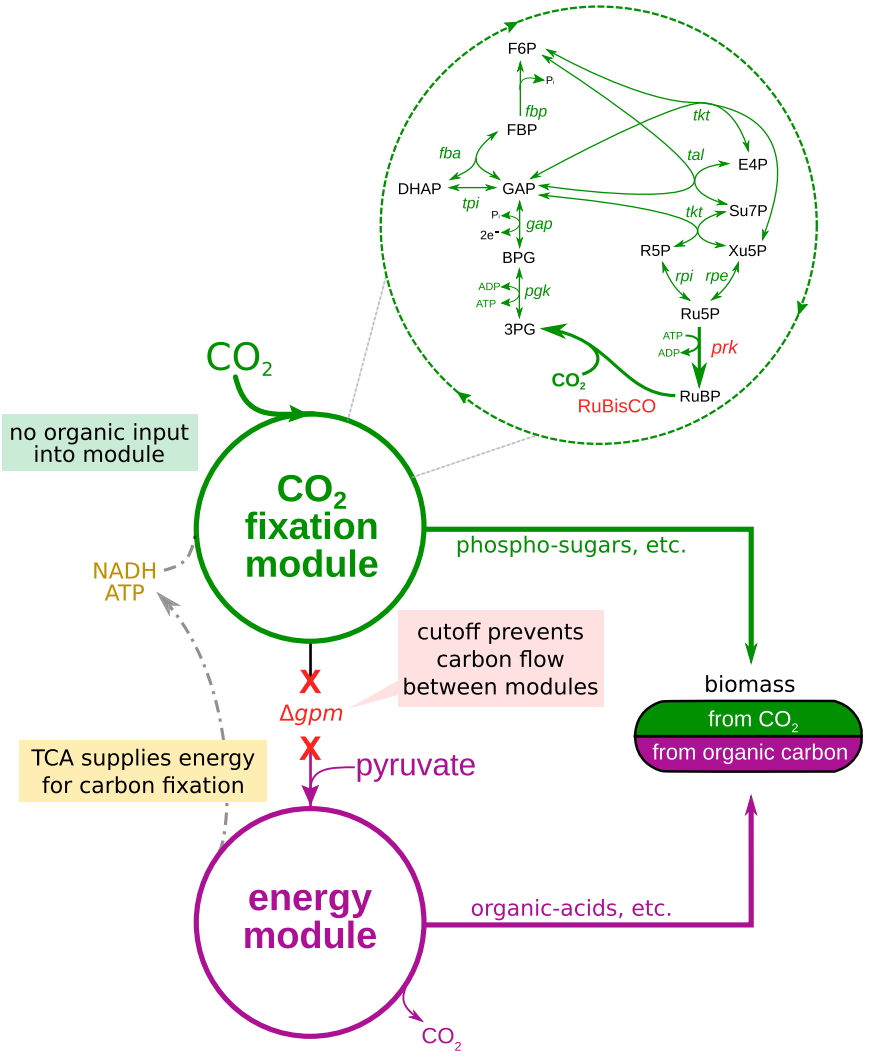

Figure 1. Decoupling Energy Production and Carbon Fixation in *E. coli* to Achieve Hemiautotrophic Growth

Two recombinant enzymes are needed to complete a carbon fixation cycle in *E. coli*: RuBisCO, the carboxylating enzyme, and the kinase prk. The remaining reactions required for the reduction and substrate regeneration phases of the cycle are endogenous to the metabolic network of the host, as part of gluconeogenesis and the pentose phosphate pathway. Deletion of the phosphoglycerate mutase genes (Δ*gpmA* and Δ*gpmM*) disrupts carbon flow in the glycolytic/gluconeogenic backbone and generates two disconnected sub-networks: (1) a carbon fixation module containing upper glycolysis, the pentose phosphate pathway, and the two foreign CBB enzymes and (2) an energy module, containing lower glycolysis and the TCA cycle, supplying reducing power and ATP. In a scenario in which an organic carbon source (e.g., pyruvate) is utilized by the energy module to supply the energetic demands of the carbon fixation cycle, the cellular building blocks derived from carbon fixation module metabolites (e.g., phospho sugars, such as ribose-P; see Figure S4 for details) can be synthesized from inorganic carbon using the non-native CBB cycle. The remainder of the biomass building blocks (those emanating from the energy module metabolites, e.g., organic acids for many of the amino acids), as well as the energy requirements of the cell, are supplied directly via the catabolism of the organic carbon source. In such a hemiautotrophic growth mode, CO_2 and energy carriers are the sole inputs for the production of biomass precursors in a carbon fixation cycle.

See also Figures S1, S2, S3, and S4.

complete carbon fixation cycle capable of autocatalytically generating biomass from CO_2 has remained an open challenge.

Here, we report achieving a fully functional and autocatalytic carbon fixation cycle in *E. coli*, capable of hexose, pentose and triose sugar synthesis with no input of organic carbon into the cycle. Energy and reducing power are supplied by the oxidation of an organic acid (pyruvate) in an isolated metabolic module and thus no net carbon gain is achieved at this point. This is the first example of a non-native carbon assimilation cycle in which all of the pathway intermediates and products are solely synthesized from CO_2 and the required co-factors.

RESULTS

Metabolic Cutoff in Gluconeogenesis Allows for the Decoupling of Energy Harvesting from Biomass Synthesis in *E. coli*

Out of the dozen of reactions utilized by autotrophs in the CBB cycle for the biosynthesis of sugars from CO_2, only two enzymatic activities are absent in *E. coli*: phosphoribulokinase (*prk*) and RuBisCO. The native enzymes of gluconeogenesis and the pentose phosphate pathway in *E. coli* can catalyze all other reactions (Figure S1). Therefore, heterologous expression of RuBisCO and *prk* could, in principle, equip *E. coli* with the enzymatic machinery needed to execute all CBB cycle reactions and achieve the synthesis of sugar, as well as other major biomass constituents, from CO_2.

Inspired by the powerful tool of genetic screens, in which genomic perturbations and controlled growth conditions are combined to identify new phenotypes, we have used a computational framework based on flux balance analysis to analyze hundreds of gene-deletion combinations and identify perturbations in central carbon metabolism that, together with RuBisCO and *prk* expression, couple the rate of carbon fixation to cellular fitness (Figures S2 and S3; Experimental Procedures). Our analysis pointed to a yet unexplored scenario in which targeted severing of gluconeogenesis would decouple energy harvesting and biomass production into two independent metabolic networks (Figure 1). This rewired metabolism could drive the synthesis of sugars and other essential biomass components from CO_2 as the sole carbon source, while production of cellular energy would be obtained from the catabolism of an organic carbon in the energy module.

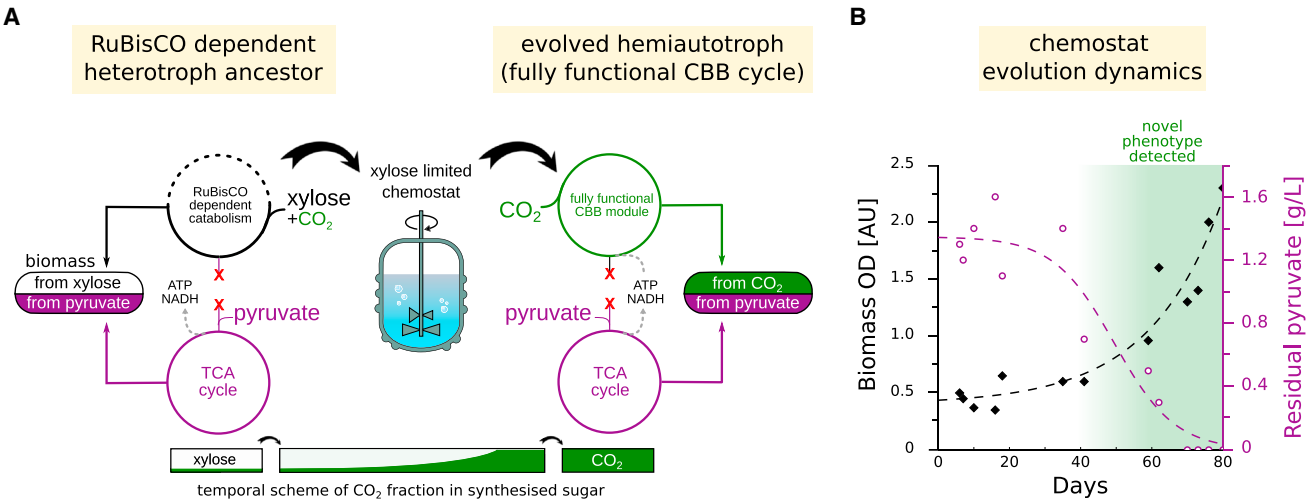

Figure 2. Chemostat Evolution Leads to a Hemiautotrophic Phenotype

(A) The ancestor strain (left) containing *gpmA and gpmM* deletions was evolved in a xylose-limited chemostat supplied with an excess of pyruvate and CO_2. Additional deletions of *pfkA*, *pfkB*, and *zwf* resulted in RuBisCO-dependent (but not hemiautotrophic) catabolism of xylose in the initial heterotrophic growth (Figure S5). Propagation in a chemostat ensured xylose-limited growth, resulting in strong selective pressure toward increased carbon fixation flux. When mutations arise that create a fully functioning CBB cycle, they enable CO_2 to be the sole carbon input for the required biomass precursors. If carbon fixation by the CBB cycle could meet cellular demand for phospho-sugars, growth dependency on xylose would be alleviated and the hemiautotrophic strain (right) could take over the population.

(B) Around day 50 of chemostat evolution, an increase in optical density (OD) (black diamonds) and a decrease in pyruvate concentration (purple circles) were observed, indicating a takeover by an evolved clone with a metabolically distinct phenotype. Culture samples from day ≈50 onward (shaded green) were able to grow in minimal media with pyruvate as the only organic carbon source in an elevated CO_2 atmosphere, both on liquid media and agar plates. Dashed lines are sigmoidal fits.

See also Figure S5.

This scenario goes beyond previously described RuBisCO-dependent strains (Gong et al., 2015; Mueller-Cajar and Whitney, 2008; Parikh et al., 2006; Zhuang and Li, 2013) by employing a fully functional autocatalytic CBB cycle in which, as in autotrophic organisms, CO_2, ATP, and reducing power are the only inputs for the synthesis of sugars. We termed this mode of growth, not known to occur in nature, hemiautotrophic growth (i.e., half-autotrophic, as it cuts metabolism into two parts, only one of which is autotrophic) and aimed to explore it in the lab. Our design for decoupling energy harvesting and CO_2 fixation does not result in a net gain of carbon when energy is obtained from the oxidation of an organic carbon source (e.g., pyruvate). However, it creates a malleable platform to test the functionality of synthetic carbon fixation pathways and offers powerful modularity in the choice of energy module for carbon fixation.

Heterologous Expression of CBB Cycle Components Is Not Sufficient to Sustain Hemiautotrophic Growth

We have experimentally followed this scenario by severing gluconeogenesis through the deletion of the phosphoglycerate mutase genes *gpmA* and *gpmM*. These deletions separate central metabolism into two disconnected sub-networks (Figure 1): (1) a carbon-fixing CBB module containing upper glycolysis, the pentose phosphate pathway, and the recombinant CBB enzymes and (2) an energy module containing lower glycolysis and the TCA cycle, which supplies ATP and reducing equivalents to power carbon fixation by the first module. Notably, all of the six cellular phospho-sugars (G6P, F6P, R5P, E4P, GAP, and 3PG) that are starting points for biosynthetic pathways diverging out of central carbon metabolism have to be synthesized completely from CO_2 by the CBB module (Figure S4). An organic-acid feeding the energy module, such as pyruvate, could provide reducing power and ATP for carbon fixation and thereby allow the synthesis of biomass precursors in the CBB module from CO_2. Importantly, our metabolic design couples the biosynthesis of sugars and other essential biomass constituents to the activity of the complete carbon fixation cycle, and not to individual enzymatic steps or sub-modules in the pathway.

In contrast to our computational prediction, a *gpm* double-deletion mutant expressing recombinant RuBisCO, *prk*, and carbonic anhydrase, provided pyruvate as a single organic carbon source, failed to grow in an elevated CO_2 atmosphere. This strain grew only when a second carbon source, a pentose sugar directly feeding the CBB module, was also provided (e.g., xylose), thus allowing biomass precursors to be synthesized from the externally supplied sugar (Figures 2A and S3D). Since our model does not account for regulatory and kinetic effects, we hypothesized that the organism failed to grow hemiautotrophically because a finely tuned flux distribution might be required, for example, to balance the rate of sugar uptake by biosynthetic pathways branching from the CBB cycle intermediates with the rate of sugar biosynthesis from CO_2 fixation.

Continuous Evolution in a Chemostat of RuBisCO-Expressing Cells Leads to Sugar Synthesis from CO_2

While rational design is limited in predicting necessary changes in regulatory or kinetic parameters, directed evolution is a powerful alternative to explore the multivariate fine-tuning required for

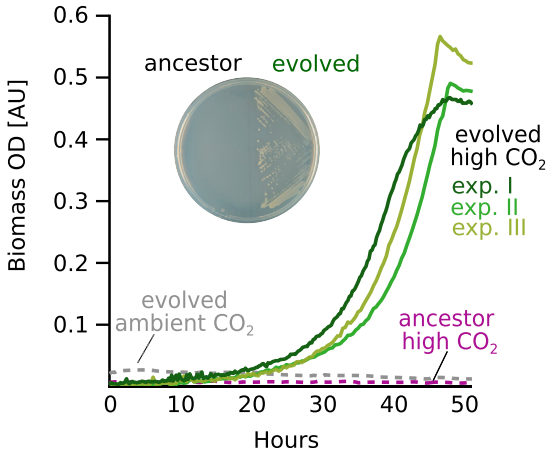

Figure 3. Growth without Xylose Is Dependent on CO_2 Availability

In contrast to the ancestral strain, evolved clones isolated from all three chemostat experiments were able to grow in minimal media, supplemented solely with pyruvate (doubling time of ≈6 hr). In all cases, growth required elevated CO_2 conditions (pCO_2 = 0.1 atm) and no growth was detected under ambient atmosphere. Similarly, evolved clones, but not the ancestral strain, were able to form colonies on minimal media agar plates when supplemented with pyruvate under a high CO_2 atmosphere (inset).

See also Figure S6.

operating non-native pathways (Sauer, 2001). Our metabolic design, which couples the biosynthesis of sugars and derived biomass components to the functionality of the non-native CBB cycle, allowed us to harness natural selection by using a chemostat-based evolution regimen that continuously maintained selective conditions for a hemiautotrophic phenotype. The ancestral strain of this evolution experiment was a double-knockout *gpm* strain expressing recombinant RuBisCO, *prk*, and carbonic anhydrase with the additional deletions of phosphofructokinase (*pfkA* and *pfkB*) and glucose-6-phosphate-1-dehydrogenase (*zwf*). Collectively, these metabolic manipulations made RuBisCO carboxylation essential for xylose catabolism during heterotrophic growth and eliminated oxidation of hexose sugars through the oxidative pentose phosphate pathway (Figure S5).

The ancestral strain was propagated in a xylose-limited chemostat (dilution rate of 0.08 h^{-1}, doubling time of ≈9 hr). The surrogate sugar (i.e., xylose) was supplied to initiate the evolutionary process, as shown in Figure 2A. We set the composition of the feed media such that the CBB module surrogate sugar ([xylose] = 0.1 g/l) became strongly limiting, and the energy module substrate was supplied in excess ([pyruvate] = 5 g/l). The scarcity of xylose in the chemostat imposes a strong and continuous selective pressure on cells to utilize the CBB cycle for sugar biosynthesis directly from the abundant inorganic carbon (i.e., CO_2) in order to alleviate the dependency on xylose. The inherent dynamics of a chemostat forces cell growth to equal the dilution rate and thus ensures that the concentration of xylose in the chemostat is extremely low and decreases even further as cells adapt. We hypothesized that this selection process will favor mutations that lead to a fully functional CBB cycle that bypasses the need for xylose, thus enabling a hemiautotrophic strain to take over the population. High levels of CO_2 (pCO_2 = 0.25 atm) were maintained throughout the experiment to maximize the RuBisCO carboxylation rate and prevent competing oxygenation reactions.

After inoculation, xylose concentration quickly fell below the detection limit (<1 mg/l) as expected for a sugar-limited chemostat regimen, while the concentration of pyruvate remained in considerable excess (≈2 g/l), as shown in Figure 2B. Due to severing gluconeogenesis by *gpm* deletion, carbon from pyruvate could not be used for sugar biosynthesis to compensate for the xylose limitation. However, excess pyruvate could potentially serve as a source of energy and reducing power to be utilized by the CBB module as it evolves to function as a xylose-independent CO_2 fixation cycle. During the first 40 days of growth (≈100 chemostat generations), we observed no significant change in cell density and nutrient concentrations in the effluent media. Over the following 20 days, we noticed a gradual increase in cell density, accompanied by a steady decrease in pyruvate concentration. Finally, around day 60 (≈150 chemostat generations; Figure 2B), the concentration of pyruvate dropped to an undetectable level (<1 mg/l), suggesting that growth was no longer limited by xylose availability and that pyruvate became fully utilized. Importantly, in contrast to the ancestral strain, culture samples from day 50 onward (Figure 2B) were able to grow in minimal media when supplied with only pyruvate and elevated CO_2 (doubling time of ≈6 hr; Figure 3). In ambient CO_2, no growth was detected in either liquid media or agar plates.

Plasmid curing from an evolved clone isolated from the chemostat resulted in the loss of the newly acquired phenotype. Cured cells lacking the RuBisCO- and *prk*-encoding plasmid did not grow in minimal media when only supplemented with CO_2 and pyruvate (Figures S6A and S6B; Experimental Procedures). We retransformed the cured strain with a modified plasmid, in which RuBisCO, *prk*, and carbonic anhydrase were placed under the control of two separate inducible promoters. Regaining the hemiautotrophic phenotype was only observed on co-induction of both enzymes (Figure S6C). This result indicates that the novel growth mode is indeed dependent on the co-expression of RuBisCO and *prk*, as expected of CBB-cycle-mediated synthesis of sugars from CO_2. We observed the evolution of clones able to grow solely on CO_2 and pyruvate in two additional independent chemostat experiments (appearing on days 60 and 130; Figures S7A–S7C; Experimental Procedures).

Mass Spectrometry Reveals that CO_2 Is the Sole Source of Carbon for Sugar Biosynthesis in the Evolved Cells

The ability of evolved bacteria to grow in the absence of xylose suggested that the CBB cycle evolved to operate in the absence of an organic input into the CBB module. To test if the intracellular pool of phospho-sugars and other CBB-cycle-derived biomass components are indeed synthesized solely from CO_2 fixation, we propagated the evolved strain in minimal media, supplemented with isotopically labeled $^{13}CO_2$ ($p^{13}CO_2$ = 0.1 atm) and non-labeled pyruvate. Isotopic labeling analysis using liquid chromatography-tandem mass spectrometry (LC-MS/MS) showed that sugars and biomass building blocks derived from the CBB module were almost completely ^{13}C-labeled, while

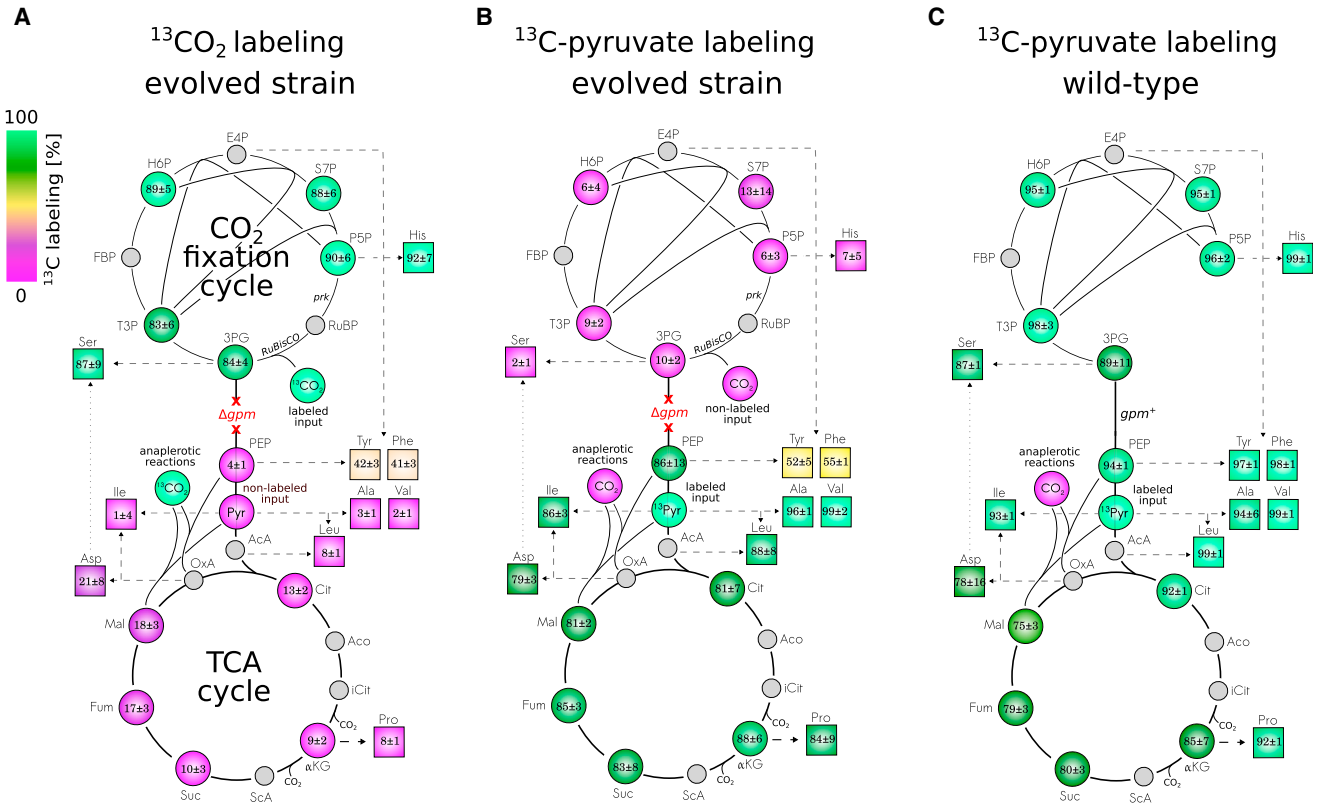

Figure 4. Isotopic Labeling Experiments Demonstrate the Biosynthesis of Sugars and Other Biomass Components from CO_2

(A) Isotopic labeling analysis, in which evolved clones were grown with isotopically labeled $^{13}CO_2$ as an inorganic carbon source and non-labeled pyruvate as an energy source, showed almost full labeling of all CBB intermediates and the derived biomass building blocks. In marked contrast, TCA intermediates and biomass components originating from the energy module show low levels of labeling, as predicted for a hemiautotrophic growth mode. This indicates that the evolved strain synthesizes CBB module biomass precursors from CO_2 using the non-native CBB cycle, while the biomass precursors originating from the energy module are synthesized from the supplemented pyruvate.

(B) In a reciprocal setup in which non-labeled CO_2 was supplied in addition to uniformly labeled pyruvate, the labeling pattern was again in agreement with hemiautotrophic growth expectations: CBB intermediates and the derived amino acids were mostly non-labeled (as the supplied CO_2), while metabolites in the energy module were mostly labeled.

(C) Metabolically unperturbed BW25113 *E. coli* in which RuBisCO and *prk* were not recombinantly expressed. As expected when lacking the *gpm* metabolic cutoff and RuBisCO, when uniformly labeled ^{13}C-pyruvate was supplied as a carbon source, the intermediates of glycolysis and the pentose-phosphate pathway were fully labeled. TCA cycle intermediates and the derived biomass components were not fully labeled due to the usage of non-labeled bicarbonate in anaplerotic reactions (denoted CO_2 for simplicity). The mean percentage (±SD) of three replicates is shown.

those derived from the energy module were almost totally unlabeled as shown in Figure 4A (Experimental Procedures). This serves as evidence of a fully functional CBB module operating in *E. coli*, capable of synthesizing sugars directly from CO_2. The labeling pattern was further verified in a reciprocal experiment in which we propagated the bacteria in the presence of uniformly labeled ^{13}C-pyruvate and unlabeled CO_2 (Figure 4B). Small deviations from homogeneous labeling of CBB produced molecules were expected due to the refixation of CO_2 released from the TCA cycle. Similarly, low levels of labeling in TCA cycle intermediates resulting from inorganic carbon usage in anaplerotic reactions can be seen in control experiments (Figures 4C, S5C, and S6D). Finally, isotopic analysis of the overall biomass content revealed that ≈35% of cellular carbon originated from CO_2 fixation (Figure S6D), matching the known fraction of biomass produced from CBB module metabolites (Neidhardt, 1987) (Figure S4).

The Only Gene Mutated in All Three Lab Evolution Experiments Is at the Main Flux Branchpoint of the CBB Cycle

To identify the mutations responsible for the emerging metabolic phenotype, we performed whole-genome sequencing of clones displaying hemiautotrophic growth, isolated from three independent evolutionary chemostat experiments (Figures S7A–S7C; Experimental Procedures). ≈80 mutational events were identified in our analysis, none of them in RuBisCO or *prk* (Tables S1, S2, and S3). Ten genes were independently mutated in more than one clone (Figure 5A), and only a single gene was mutated in all three experiments. This gene, ribose-phosphate diphosphokinase *(prs)*, encodes for an enzyme that phosphorylates ribose-5-phosphate and is the main flux branchpoint of the CBB module in which a pentose sugar is diverted toward biomass production. All three mutations were within the coding sequence: two of which were missense mutations (A95T and

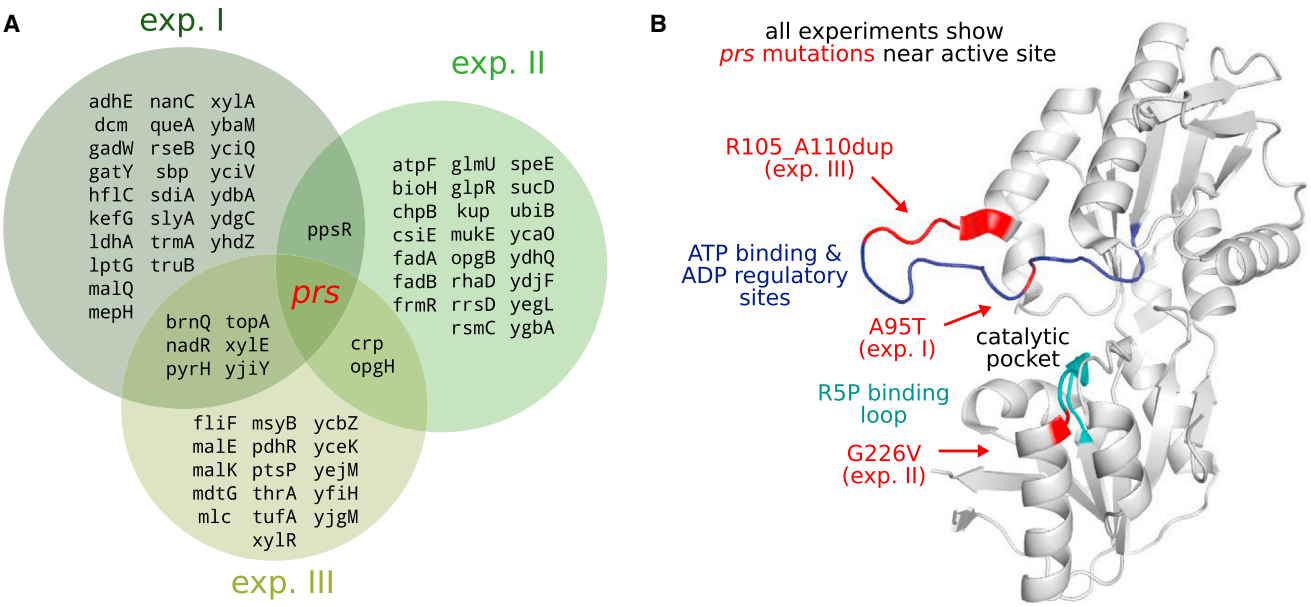

Figure 5. The Genetic Basis Underlying the Hemiautotrophic Phenotype

(A) Venn diagram summarizing the intersection among mutations accumulated in hemiautotrophic evolved strains isolated from three distinct chemostat experiments. A detailed description of the mutations can be found in Tables S1, S2, and S3. In the ancestral strain for the second chemostat experiment (exp. II) a Δ*mutS* deletion that induces hyper-mutability was introduced (only mutations occurring between chemostat inoculation and hemiautotrophic phenotype emergence are depicted).

(B) Ribose-phosphate diphosphokinase (*prs*), the main flux branching enzyme of the CBB module by which ribose-phosphate is diverted toward biomass production, was the only gene in which mutations appeared in all of the chemostat evolution experiments. Structural analysis (based on the most closely available crystal structure, that of *Bacillus subtilis* showing ≈70% sequence similarity to the *E.coli* homolog) indicates that the mutations are located in catalytically active regions of the enzyme, either on the ribose-5-phosphate substrate binding loop (turquoise) or on a second loop containing the ATP binding site and an allosteric regulatory site (dark blue).

See also Figure S7 and Tables S1, S2, and S3.

G226V), and the third was an 18-bp tandem duplication, leading to in-frame insertion of six amino acids (R105_A110dup). Structural analysis showed that all *prs* mutations arose within loops participating in substrate binding and catalytic activity (Figure 5B) (Eriksen et al., 2000). When the *prs* wild-type sequence was reintroduced to the evolved genetic background (Experimental Procedures), replacing the mutated *prs* sequence, the phenotype was lost: growth was only observed when xylose was supplemented in addition to pyruvate and CO_2, as in the ancestral strain. Given that *prs* is the main branchpoint in which a pentose sugar is shunted from the CBB cycle toward biomass, we hypothesized that a change in one or more of the enzymatic parameters of *prs* was required for CBB cycle operation as discussed in the next section.

The rate of mutation accumulation identified in the evolved hemiautotrophic strains exceeds those reported in previous adaptive evolution studies (Barrick et al., 2009; Foster et al., 2015). This can be the result of several contributing factors, such as the known increased mutation rate under carbon starvation (Notley-McRobb et al., 2003; Novick and Szilard, 1950). Similarly, the tailored selective conditions we have used give ample ground for beneficial mutations that can (partially) restore fitness and shift the evolutionary dynamics toward a "strong selection, strong mutation" regime (Desai and Fisher, 2007) in which successive mutational sweeps and mutational cohorts are known to lead to relatively fast fixation of mutations. Interestingly, we note a bias in the spectrum of fixed mutations in some of the strains isolated from distinct experiments (Tables S1, S2, and S3). The underlying basis of this observation is currently unclear. In terms of copy number of the plasmid harboring RuBisCO and *prk*, we did not observe any consistent variations in the evolved strains versus the ancestor and the plasmid sequence did not show any mutations (Experimental Procedures).

Modeling the Autocatalytic Carbon Fixation Cycle Suggests that Fine-Tuning of *prs* Catalytic Rate Is Essential for Metabolic Stability

In contrast to linear metabolic pathways in which stable metabolic steady-state can be achieved, regardless of the specific kinetic properties, the stability of autocatalytic cycles (consisting of a set of metabolites which regenerate more of themselves with each turn of the cycle) is not guaranteed. The stability depends on the topology of the cycle and the kinetic parameters of the enzymes involved (Reznik and Segrè, 2010). This is demonstrated in the simplified model shown in Figure 6A, consisting of an autocatalytic effective carbon fixation reaction (ν_{CBB}) and a biomass generating reaction (ν_{prs}) from which assimilated carbon is shunted toward biosynthesis. The stability of the steady state in this metabolic network depends on the kinetic properties of the enzymes, as these parameters govern

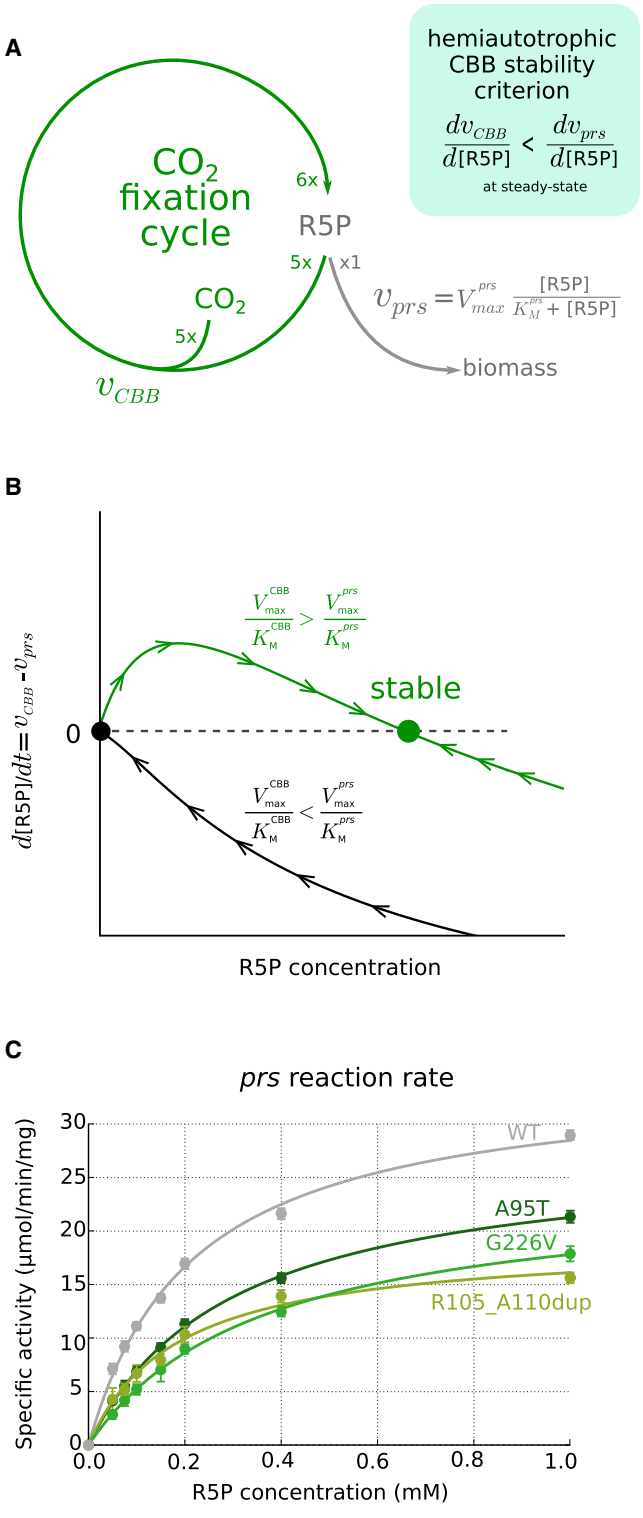

Figure 6. Stability Analysis of Autocatalytic Carbon Fixation Cycles

(A) Simplified model for an autocatalytic carbon fixation cycle. We consider a two-reaction pathway in which a generalized carbon fixation reaction autocatalytically produces a metabolite (R5P) from an external supply of CO_2 (effectively performing five carboxylations, $v_{CBB} = v_{RuBisCO}/5$). A second reaction consumes R5P for the production of biomass. For clarity, we assume irreversible Michaelis-Menten rate laws. Model parameters for each reaction are the Michaelis constant (K_M) and the maximal reaction rate ($V_{max} = [E] \cdot k_{cat}$, where [E] is the enzyme concentration and k_{cat} is the turnover number). For a steady-state concentration to be stable, the derivative of v_{prs} with respect to R5P concentration has to be higher than the derivative of v_{CBB} at the steady-state point. This relation will imply that if R5P concentration deviates from its steady state, the flux through the reaction branching to biomass synthesis would stabilize the R5P concentration. In terms of metabolic control analysis, this is equivalent to requiring that the elasticity of the *prs* reaction is greater than the elasticity of the CBB reaction at the steady-state point.

(B) Schematic of the stability analysis in the phase space of R5P concentration showing the net flux at the branchpoint. The steady-state concentration of R5P (inferred from setting $v_{CBB} = v_{prs}$) and the stability of the steady state are determined by values of the parameters. Assuming the maximal rate of carbon fixation is lower than biomass synthesis ($V_{max}^{CBB} < V_{max}^{prs}$), a non-zero stable steady state exists if the enzymatic parameters of *prs* satisfy the relation $(V_{max}^{CBB}/K_M^{CBB}) > (V_{max}^{prs}/K_M^{prs})$.

(C) Experimental in vitro reaction rate measurements of purified *prs* enzymes, with either wild-type or mutated sequences. All of the mutated *prs* enzymes from the evolved strains show ≈2-fold decrease in their k_{cat}/K_M values, as predicted by the stability analysis. The measured values in respect to the wild-type enzyme were 57% ± 2%, 65% ± 6%, and 38% ± 3% for the A95T, G226V, and R105_A110dup *prs* mutations, respectively. The mean percentage (±SD) of three replicates is shown.

the response to a perturbation in the intracellular concentration of the metabolite at the flux branchpoint. Explicitly, for a stable steady state to exist in the carbon fixation cycle, the Michaelis constant of *prs* must satisfy: $(V_{max}^{CBB}/K_M^{CBB}) > (V_{max}^{prs}/K_M^{prs})$ (where $V_{max} = [E] \cdot k_{cat}$ and V_{max}^{CBB} and K_M^{CBB} are effective parameters that are a function of all the reactions composing the CBB cycle). This relation ensures that enough flux remains in the cycle to ensure autocatalysis (Figure 6B; Supplemental Experimental Procedures).

In order to test the model prediction, we measured in vitro the reaction rates of mutated *prs* toward its substrate ribose-5-phosphate. In all cases, as shown in Figure 6C, we found an approximately 2-fold decrease in $(k_{cat}^{prs}/K_M^{prs})$ following the evolutionary process, consistent with the stability analysis requirement (Experimental Procedures; no changes were observed in the *Prs* protein expression levels). This observation of convergent evolution strengthens the hypothesis that, in addition to the expression of recombinant CBB cycle enzymes, changes in the kinetic properties of endogenous components, which interact with the non-native pathway, are essential for a stably operating carbon fixation cycle and hence for the hemiautotrophic phenotype to emerge. We found that a mutated *prs* was not sufficient to allow hemiautotrophic growth when introduced on the ancestral strain background (Experimental Procedures), demonstrating that while fine-tuning of fluxes at the flux branchpoint via the *prs* mutation is essential, this mutation alone is not sufficient to fully reconstruct the phenotype.

To further identify endogenous metabolic components that require fine-tuning to achieve stable operation of the carbon fixation pathway, we conducted a fourth chemostat evolution experiment (Figure S7D), in which one of the observed *prs* mutations (R105_A110dup) was introduced to the genetic background of the ancestral strain. In addition, we knocked out the PEP synthase regulatory protein (*ppsR*), as this gene is the only shared mutation between experimental repeats I and II

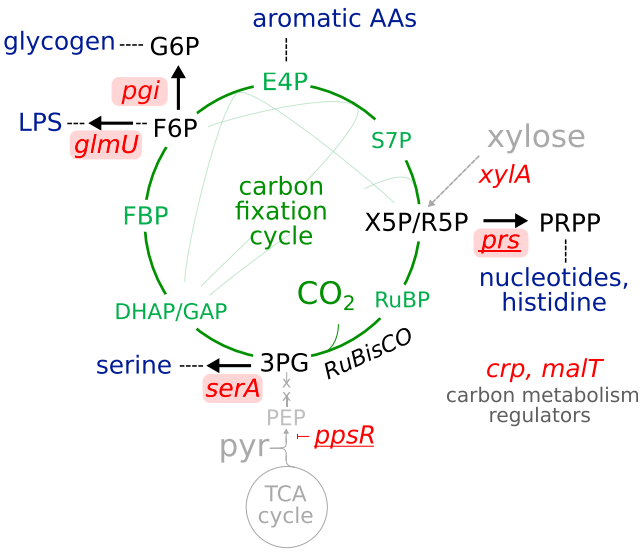

Figure 7. Acquired Mutations Focus on Flux Branchpoints and Carbon Metabolism Regulators

A fourth evolution experiment was initialed with a modified ancestral strain, containing additional mutations in *prs* (R105_A110dup, underlined) and *ppsR* (knockout, underlined). Emergence of the hemiautotrophic phenotype was detected in <100 chemostat generations. Whole-genome sequencing of isolated clones revealed that six mutations, in addition to *prs* and *ppsR*, were acquired in the evolutionary transition toward hemiautotrophic growth (red). Out of a total of eight mutations appearing in this hemiautotrophic strain, four are found in flux branchpoints, shunting cycle intermediates toward biomass (*serA*, *pgi*, and *glmU* in addition to *prs*), an additional three are in regulators of carbon metabolism (*crp*, *malT*, and *ppsR*), and one (*xylA*) is in the catabolism of the surrogate xylose sugar not used by the final evolved phenotype. A detailed description of the mutations can be found in Table S4.

See also Table S4.

beyond *prs* (Experimental Procedures). While the introduction of these two mutations to the ancestral background was not sufficient to achieve hemiautotrophic growth, xylose-limited chemostat evolution (dilution rate of 0.035 h^{-1}) rapidly led to the emergence of a hemiautotrophic phenotype in <100 chemostat generations (Figure S7D). Whole-genome sequencing of hemiautotrophic clones isolated from this chemostat experiment revealed that six mutations were fixed in the evolutionary process (Figure 7; Table S4). Strikingly, almost all of the newly acquired mutations appeared in either flux branching points toward biomass from the CBB cycle (*serA*, *pgi*, and *glmU*) or global regulators of carbon metabolism (*crp* and *malT*). Four out of these six loci were mutated in at least one previous experiment (*crp*, *glmU*, *xylA*, and the *mal* operon). These results demonstrate that the functionality of the non-native CBB cycle depends not only on the introduction of heterologous enzymes required to construct the pathway but also on the fine-tuning of endogenous components interacting with it, mostly biosynthetic enzymes feeding from the carbon pool of the cycle (Figure 7).

DISCUSSION

While several synthetic metabolic pathways have been successfully integrated into model microorganisms, such as *E. coli* and *S. cerevisiae*, the introduction of an autocatalytic carbon fixation pathway into a heterotrophic host has remained a standing challenge (Müller et al., 2015; Siegel et al., 2015). In this study, we demonstrate that the combination of rational design and laboratory evolution can rapidly evolve a strain to convert CO_2 into sugars and other biomass components via non-native carbon fixation machinery. The striking ability of *E. coli* to rapidly change its growth mode demonstrates that central carbon metabolism can be extremely adaptive when subjected to selective conditions and extends the possibilities for achieving novel metabolic phenotypes. Successful introduction of carbon fixation into a heterotrophic model organism suggests that closely related radical modulations of C1 central carbon metabolism, such as the desired synthetic methylotrophy (Whitaker et al., 2015), synthetic mixotrophy (Fast et al., 2015), and synthetic electrotrophy (Lovley, 2011), can be well within reach with a similar approach. From an industrial perspective, even though not translated to immediate industrial applications, a fully functional non-native CO_2 fixation cycle is a critical milestone toward synthetic lithoautotrophy. Our strategy to decouple energy and carbon fixation metabolism enables powerful modularity in the choice of energy module used to energize the synthetic cycle. The methodology we present of selection-based evolutionary transitions can be directly extended to establish a synthetic methylotrophic strain, utilizing industrially relevant energy sources, such as methanol, to drive CO_2 fixation. Furthermore, previous studies described the "paper biochemistry" of several fully synthetic carbon fixation cycles, not known to occur in nature, with promising predicted kinetic properties (Bar-Even et al., 2010). Our results suggest an experimental route to implement these pathways in a fast growing, genetically malleable model organism, such as *E. coli.*

In contrast to a traditional design scheme, in which individual components or sub-modules are tested and then integrated, our metabolic design focused on the coupling of cellular fitness to the desired functionality. While the initial rational design, arising from our in silico analysis, was not sufficient to achieve the desired phenotype, it formed the genetic basis and suggested the selective conditions under which a complex metabolic transition evolved. The ability to create synergy between rational metabolic design and laboratory evolution by tailoring the appropriate experimental setup is essential for harnessing natural selection to fine-tuning the metabolic network. Quantitative a priori prediction of the interactions between endogenous and newly introduced metabolic functions is often challenging due to the lack of sufficient information regarding the kinetics, energetics, and regulation of the relevant components. A design that couples cellular fitness to the activity of a non-native pathway is therefore useful. Such coupling allows the harnessing of natural selection in a controlled environment to obtain the necessary fine-tuning between native and non-native metabolic functions to achieve the desired phenotype. Since chemostats inherently implement a feedback mechanism that continuously increases the selection stringency in response to improvements in the desired pathway activity, they can serve as an ideal platform for evolving pathways that utilize non-native substrates, such as inorganic carbon. A dynamic selection stringency, as in the case of chemostats, enables growth during the early phases of

laboratory evolution by supplying limiting amounts of a surrogate sugar (i.e., xylose), which compensates for the lack of full pathway activity, even if the carbon fixation pathway performs suboptimally (Kleeb et al., 2007).

The hybrid approach demonstrated here of rational design combined with laboratory evolution has allowed us, for the first time, to achieve a fully functional carbon fixation cycle in a heterologous host. Our results make evident the remarkable plasticity of metabolism and provide a malleable platform for deciphering the biochemistry and evolution of carbon fixation. The rapid emergence of a novel metabolic phenotype in laboratory timescales suggests a route for synthetic biology efforts to optimize pathways of biotechnological importance that can drive transformative advances in our ability to tackle the grand challenge of resource sustainability in years to come.

EXPERIMENTAL PROCEDURES

Strains and Genomic Modifications

An *E. coli BW25113* strain (Grenier et al., 2014), referred to in the text as "wild-type," was used as the parental strain for further genomic modifications. The genome sequence of the parent used for constructing the ancestor strain differed from the *E. coli* strain *BW25113* at four loci*: ptsI (D464N)*, *fabR (V42G)*, *btuB (G162A)*, and *fhuA (frameshift).* These mutations were acquired during early handling of the strain prior to chemostat inoculation. The strain inoculated in the chemostat for the evolutionary experiment, referred to in the text as "ancestor," contained further genomic modifications: we deleted phosphoglycerate mutase genes (*gpmA* and *gpmM*), phosphofructokinase genes (*pfkA* and *pfkB*), and 6-phosphate-1-dehydrogenase (*zwf*). In addition, we further deleted the *aceBAK* operon encoding for the enzymes of the glyoxylate shunt, thus ensuring that a bypass using the tartronate semialdehyde pathway cannot be used to grow on pyruvate as a sole organic carbon source in Δ*gpm* mutant. A detailed description of the methods used for performing genomic modifications can be found in the Supplemental Experimental Procedures. The ancestral strain inoculated in the second chemostat experiment contained a Δ*mutS* mutation that induces hyper-mutability. Detailed information regarding the genotype of clones showing hemiautotrophic phenotype, referred to in the text as "evolved isolated clones," appears in Tables S1, S2, S3, and S4.

Recombinant Expression of RuBisCO, prk, and Carbonic Anhydrase

For recombinant expression of the CBB cycle components, we constructed a synthetic operon encoding the His-tagged type II RuBisCO (*cbbM*) from *Rhodospirillum rubrum ATCC 11170* (courtesy of Prof. Michal Shapira), His-tagged phosphoribulokinase (*prkA*) from *Synechococcus elongatus PCC 7942* (courtesy of Prof. Ichiro Matsumura), and carbonic anhydrase (Rru_A2056) from *Rhodospirillum rubrum* (*CA*). Synthetic ribosomal binding sites were used to achieve different levels of expression, as previously described (Zelcbuch et al., 2013). The synthetic operon was cloned into a pZA11 expression vector (Expressys). Detailed information regarding the construction and sequence of the plasmid containing the synthetic operon (pCBB), plasmid curing, and the reintroduction of modified plasmids can be found in the Supplemental Experimental Procedures.

Growth Conditions

Cells were grown on M9 minimal media, supplemented with 34 mg/l chloramphenicol and suitable carbon sources, as specified in the text. Agar plates were prepared using ultrapure agarose (Hispanagar). Growth curves were obtained by culturing cells in 96-well plates incubated at 37°C in a gas-controlled shaking incubator (Infinite M200, Tecan). In experiments in which frozen bacterial stock was used to inoculate the culture (e.g., $^{13}CO_2$ labeling experiments), cells were first streaked on solid minimal media supplemented with pyruvate (0.5%) and xylose (0.1%) to facilitate initial growth. Several colonies were then streaked on solid minimal media supplemented with pyruvate. Once growth was observed, liquid minimal medium supplemented only with pyruvate was inoculated. We found that, in order to achieve the transition between xylose containing medium and pyruvate alone, it was required to sample several colonies to ensure hemiautotrophic growth initiation. All growth was performed in enriched CO_2 atmosphere (pCO_2 = 0.1 atm).

Computational Analysis of RuBisCO-Dependent Strains

To computationally identify candidate mutants in which cell growth is coupled to the flux through non-native CBB enzymes, we implemented an algorithm based on the principles of flux balance analysis (FBA) (Orth et al., 2010). We started by considering combinations of up to three enzymatic reaction knockouts in central metabolism and filtered out all those combinations that allow growth without any flux in RuBisCO. For those that cannot produce any biomass without RuBisCO, we calculated a slope defined as the biomass production rate achieved by allowing a unit of flux in RuBisCO. All other constraints were the same as in standard FBA, where the rate of biomass production is maximized. Details regarding software implementation can be found in the Supplemental Experimental Procedures.

Chemostat Evolution

Chemostat-based laboratory evolution was conducted in four independent experiments. Gas inflow composition was 25% CO_2, 5% O_2, and 70% N_2 and temperature was maintained at 37°C. We used Bioflo 110 chemostats (New Brunswick Scientific) with a working volume of 0.7 l except in the second experiment, which used a DASBox bacterial fermentation system (DASGIP) with a working volume of 0.1 l. In the first and third experiments, the dilution rate was set to 0.08 h^{-1} (equivalent to 9 hours of doubling time) with a feed input of M9 minimal media supplemented with 5 g/l sodium pyruvate, 100 mg/l xylose, and 34 mg/l chloramphenicol. In the second and fourth experiments, the dilution rate was set to 0.035 h^{-1} (equivalent to 20 hours of doubling time) with a feed input of M9 minimal media supplemented with 5 g/l sodium pyruvate, 25 mg/l xylose, and 34 mg/l chloramphenicol.

Isotopic Labeling Experiments

For mass isotopologues distribution analysis, cells were cultured in M9 minimal media, either in the presence of a uniformly labeled ^{13}C-pyruvate and unlabeled CO_2 or in a reciprocal setup with isotopically labeled $^{13}CO_2$ (Cambridge Isotope Laboratories) and a non-labeled pyruvate. For experiments in which gaseous $^{13}CO_2$ was used, culture tubes were placed in a transparent air-tight container and flushed with five volumes of isotopically labeled gas mixture (10% $^{13}CO_2$, 10% O_2, and 80% N_2). Cells were incubated in a shaking incubator at 37°C and harvested during exponential growth. For the extraction of intracellular metabolites, we used cold (−20°C) acetonitrile:methanol:water (40:40:20) extraction solution. A ZIC-pHILIC column (4.6 × 150 mm, guard column 4.6 × 10 mm; Merck) was used for liquid chromatography separation using gradient elution with a solution of 20 mM ammonium carbonate, with 0.1% ammonium hydroxide and acetonitrile at 0.1 ml/min. Detection of metabolites was performed using a Thermo Scientific Exactive high-resolution mass spectrometer with electrospray ionization, examining metabolites in a polarity switching mode over the mass range of 75–1,000 *m/z*. Compound identities were verified by matching masses and retention times to authenticated standards library. In addition we analyzed the labeling of proteinogenic amino acids obtained from the acid hydrolysis of protein biomass as described in the Supplemental Experimental Procedures. Data analysis was performed using TargetLynx (Waters) and the Maven software suite (Melamud et al., 2010). Total carbon labeling was calculated according to the formula:

$$labeled\ fraction = \frac{\sum_{i=0}^{n} m_i * i}{\sum_{i=0}^{n} m_i * n}.$$

Further details and the description for the measurement of isotopic carbon ratio in whole-biomass samples can be found in the Supplemental Experimental Procedures.

Whole-Genome Sequencing and Analysis

DNA was extracted from sampled cultures using a DNeasy Blood and Tissue Kit (QIAGEN), and sequencing was performed using an Illumina Hiseq 2500

platform. Detailed information regarding sample preparation can be found in the Supplemental Experimental Procedures. A reference genome was constructed based on the *E. coli* strain BW25113 (Grenier et al., 2014) and the sequence of the CBB enzymes encoding plasmid as a second contig. Sequence alignment and variant calling was achieved by use of the breseq pipeline (Deatherage and Barrick, 2014). The breseq program was used to identify genomic variants, including SNPs and insertion-deletion polymorphisms (INDELs). We note that our analysis does not capture certain types of mutations, such as copy number variations.

SUPPLEMENTAL INFORMATION

Supplemental Information includes Supplemental Experimental Procedures, seven figures, and four tables and can be found with this article online at http://dx.doi.org/10.1016/j.cell.2016.05.064.

AUTHOR CONTRIBUTIONS

A.B.-E., N.A., E.N., and R.M. designed the project; N.A., L.Z., E.H., T.B., and S.A. constructed the plasmids and performed genome engineering; E.N., U.B., N.T., N.A., A.W., D.D., and A.B.-E. developed the computational framework; N.A., S.G., Y.Z., E.H., S.A., S.M., G.J., T.B., I.S., and D.G.W. performed the experiments; N.A., S.G., E.N., and S.M. performed and analyzed LC-MS/MS experiments; S.G. and Y.Z. generated the sequencing data; N.A., S.G., Y.B., and U.B. analyzed the sequencing data; and N.A., S.G., A.B.-E., and R.M. wrote the paper.

ACKNOWLEDGMENTS

We thank Ichiro Matsumura for kindly supplying the prkA plasmid and Michal Shapira for kindly supplying the *R. rubrum* culture. We also thank Amir Aharoni, Asaph Aharoni, Uri Alon, Gil Amitai, Abdussalam Azem, Naama Barkai, Sima Benjamin, Sonjia Billerbeck, Dvora Biran, Elad Chomski, Ahuva Cooperstein, Daniel Dar, Michal Dayagi, Shani Doron, Noa Dvir, Avigdor Eldar, David Fell, Avi Flamholz, Shay Fleishon, Idan Frumkin, Shlomit Gilad, Pierre Goloubinoff, Michael Gurevitz, Jacob Hanna, Tami Hayon, Lee-Or Herzog, Keren Kahil, Miriam Kaltenbach, Mechael Kanovsky, Aaron Kaplan, Leeat Keren, Roy Kishony, Hagar Kroytoro, Rob Last, Paola Laurino, Tali Lavy, Ronen Levi, Ayelet Levin, Yishai Levin, Avi Levy, Hannes Link, Adar Lopez, Yehuda Marcus, Barak Marcus, Adi Millman, Uri Moran, Oliver Mueller-Cajar, Yotam Nadav, Amnon Naziri, Ravit Netzer, Gal Ofir, Nigel Orme, Rob Phillips, Uri Pick, Noa Rippel, Orel Rivni, Liat Rockah, Ilana Rogachev, Eliora Ron, Dave Savage, Alon Savidor, Efrat Schwartz, Lior Shachar, Tali Shalit, Tomer Shlomi, Rotem Sorek, Zvika Tamari, Dan Tawfik, Noam Vardi, Adi Volpert, Alon Wellner, Sagit Yahav, Dan Yakir, Oren Yishai, and Yonatan Zegman for support and feedback on this research. This work was funded by the European Research Council (projects SYMPAC 260392 and NOVCARBFIX 646827), Dana and Yossie Hollander, the Helmsley Charitable Foundation, the Larson Charitable Foundation, the Estate of David Arthur Barton, the Anthony Stalbow Charitable Trust, and Stella Gelerman, Canada. R.M. is the Charles and Louise Gartner professional chair and an EMBO young investigator program member. D.G.W. is supported by the United States-Israel Education Foundation.

Received: December 15, 2015
Revised: March 2, 2016
Accepted: May 17, 2016
Published: June 23, 2016

REFERENCES

Bar-Even, A., Noor, E., Lewis, N.E., and Milo, R. (2010). Design and analysis of synthetic carbon fixation pathways. Proc. Natl. Acad. Sci. USA *107*, 8889–8894.

Bar-Even, A., Noor, E., and Milo, R. (2012). A survey of carbon fixation pathways through a quantitative lens. J. Exp. Bot. *63*, 2325–2342.

Barrick, J.E., Yu, D.S., Yoon, S.H., Jeong, H., Oh, T.K., Schneider, D., Lenski, R.E., and Kim, J.F. (2009). Genome evolution and adaptation in a long-term experiment with Escherichia coli. Nature *461*, 1243–1247.

Bassham, J.A., Benson, A.A., Kay, L.D., Harris, A.Z., Wilson, A.T., and Calvin, M. (1954). The path of carbon in photosynthesis. XXI. The cyclic regeneration of carbon dioxide acceptor1. J. Am. Chem. Soc. *76*, 1760–1770.

Blount, Z.D., Borland, C.Z., and Lenski, R.E. (2008). Historical contingency and the evolution of a key innovation in an experimental population of Escherichia coli. Proc. Natl. Acad. Sci. USA *105*, 7899–7906.

Church, G.M., Elowitz, M.B., Smolke, C.D., Voigt, C.A., and Weiss, R. (2014). Realizing the potential of synthetic biology. Nat. Rev. Mol. Cell Biol. *15*, 289–294.

Deatherage, D.E., and Barrick, J.E. (2014). Identification of mutations in laboratory-evolved microbes from next-generation sequencing data using breseq. Methods Mol. Biol. *1151*, 165–188.

Desai, M.M., and Fisher, D.S. (2007). Beneficial mutation selection balance and the effect of linkage on positive selection. Genetics *176*, 1759–1798.

Durão, P., Aigner, H., Nagy, P., Mueller-Cajar, O., Hartl, F.U., and Hayer-Hartl, M. (2015). Opposing effects of folding and assembly chaperones on evolvability of Rubisco. Nat. Chem. Biol. *11*, 148–155.

Eriksen, T.A., Kadziola, A., Bentsen, A.K., Harlow, K.W., and Larsen, S. (2000). Structural basis for the function of Bacillus subtilis phosphoribosyl-pyrophosphate synthetase. Nat. Struct. Biol. *7*, 303–308.

Fast, A.G., Schmidt, E.D., Jones, S.W., and Tracy, B.P. (2015). Acetogenic mixotrophy: novel options for yield improvement in biofuels and biochemicals production. Curr. Opin. Biotechnol. *33*, 60–72.

Foster, P.L., Lee, H., Popodi, E., Townes, J.P., and Tang, H. (2015). Determinants of spontaneous mutation in the bacterium Escherichia coli as revealed by whole-genome sequencing. Proc. Natl. Acad. Sci. USA *112*, E5990–E5999.

Fuchs, G. (2011). Alternative pathways of carbon dioxide fixation: insights into the early evolution of life? Annu. Rev. Microbiol. *65*, 631–658.

Galanie, S., Thodey, K., Trenchard, I.J., Filsinger Interrante, M., and Smolke, C.D. (2015). Complete biosynthesis of opioids in yeast. Science *349*, 1095–1100.

Gong, F., Liu, G., Zhai, X., Zhou, J., Cai, Z., and Li, Y. (2015). Quantitative analysis of an engineered CO2-fixing Escherichia coli reveals great potential of heterotrophic CO2 fixation. Biotechnol. Biofuels *8*, 86.

Grenier, F., Matteau, D., Baby, V., and Rodrigue, S. (2014). Complete genome sequence of Escherichia coli BW25113. Genome Announc. *2*, e01038-14.

Kleeb, A.C., Edalat, M.H., Gamper, M., Haugstetter, J., Giger, L., Neuenschwander, M., Kast, P., and Hilvert, D. (2007). Metabolic engineering of a genetic selection system with tunable stringency. Proc. Natl. Acad. Sci. USA *104*, 13907–13912.

Li, H., Opgenorth, P.H., Wernick, D.G., Rogers, S., Wu, T.-Y., Higashide, W., Malati, P., Huo, Y.-X., Cho, K.M., and Liao, J.C. (2012). Integrated electromicrobial conversion of CO2 to higher alcohols. Science *335*, 1596.

Lin, M.T., Occhialini, A., Andralojc, P.J., Parry, M.A.J., and Hanson, M.R. (2014). A faster Rubisco with potential to increase photosynthesis in crops. Nature *513*, 547–550.

Lovley, D.R. (2011). Powering microbes with electricity: direct electron transfer from electrodes to microbes. Environ. Microbiol. Rep. *3*, 27–35.

Maddamsetti, R., Lenski, R.E., and Barrick, J.E. (2015). Adaptation, clonal interference, and frequency-dependent interactions in a long-term evolution experiment with Escherichia coli. Genetics *200*, 619–631.

Melamud, E., Vastag, L., and Rabinowitz, J.D. (2010). Metabolomic analysis and visualization engine for LC-MS data. Anal. Chem. *82*, 9818–9826.

Mueller-Cajar, O., and Whitney, S.M. (2008). Evolving improved Synechococcus Rubisco functional expression in Escherichia coli. Biochem. J. *414*, 205–214.

Müller, J.E.N., Meyer, F., Litsanov, B., Kiefer, P., Potthoff, E., Heux, S., Quax, W.J., Wendisch, V.F., Brautaset, T., Portais, J.-C., and Vorholt, J.A. (2015). Engineering Escherichia coli for methanol conversion. Metab. Eng. *28*, 190–201.

Neidhardt F.C., ed. (1987). *Escherichia coli* and Salmonella typhimurium: cellular and molecular biology, volumes I and II (American Society for Microbiology).

Notley-McRobb, L., Seeto, S., and Ferenci, T. (2003). The influence of cellular physiology on the initiation of mutational pathways in Escherichia coli populations. Proc. Biol. Sci. *270*, 843–848.

Novick, A., and Szilard, L. (1950). Experiments with the chemostat on spontaneous mutations of bacteria. Proc. Natl. Acad. Sci. USA *36*, 708–719.

Orth, J.D., Thiele, I., and Palsson, B.Ø. (2010). What is flux balance analysis? Nat. Biotechnol. *28*, 245–248.

Parikh, M.R., Greene, D.N., Woods, K.K., and Matsumura, I. (2006). Directed evolution of RuBisCO hypermorphs through genetic selection in engineered E.coli. Protein Eng. Des. Sel. *19*, 113–119.

Quandt, E.M., Gollihar, J., Blount, Z.D., Ellington, A.D., Georgiou, G., and Barrick, J.E. (2015). Fine-tuning citrate synthase flux potentiates and refines metabolic innovation in the Lenski evolution experiment. eLife *4*, e09696, pii.

Reznik, E., and Segrè, D. (2010). On the stability of metabolic cycles. J. Theor. Biol. *266*, 536–549.

Sauer, U. (2001). Evolutionary engineering of industrially important microbial phenotypes. Adv. Biochem. Eng. Biotechnol. *73*, 129–169.

Shih, P.M., Zarzycki, J., Niyogi, K.K., and Kerfeld, C.A. (2014). Introduction of a synthetic CO_2-fixing photorespiratory bypass into a cyanobacterium. J. Biol. Chem. *289*, 9493–9500.

Siegel, J.B., Smith, A.L., Poust, S., Wargacki, A.J., Bar-Even, A., Louw, C., Shen, B.W., Eiben, C.B., Tran, H.M., Noor, E., et al. (2015). Computational protein design enables a novel one-carbon assimilation pathway. Proc. Natl. Acad. Sci. USA *112*, 3704–3709.

Whitaker, W.B., Sandoval, N.R., Bennett, R.K., Fast, A.G., and Papoutsakis, E.T. (2015). Synthetic methylotrophy: engineering the production of biofuels and chemicals based on the biology of aerobic methanol utilization. Curr. Opin. Biotechnol. *33*, 165–175.

Wiser, M.J., Ribeck, N., and Lenski, R.E. (2013). Long-term dynamics of adaptation in asexual populations. Science *342*, 1364–1367.

Yim, H., Haselbeck, R., Niu, W., Pujol-Baxley, C., Burgard, A., Boldt, J., Khandurina, J., Trawick, J.D., Osterhout, R.E., Stephen, R., et al. (2011). Metabolic engineering of Escherichia coli for direct production of 1,4-butanediol. Nat. Chem. Biol. *7*, 445–452.

Zelcbuch, L., Antonovsky, N., Bar-Even, A., Levin-Karp, A., Barenholz, U., Dayagi, M., Liebermeister, W., Flamholz, A., Noor, E., Amram, S., et al. (2013). Spanning high-dimensional expression space using ribosome-binding site combinatorics. Nucleic Acids Res. *41*, e98.

Zhuang, Z.-Y., and Li, S.-Y. (2013). Rubisco-based engineered Escherichia coli for in situ carbon dioxide recycling. Bioresour. Technol. *150*, 79–88.